Effect of ginkgolide K on calcium channel activity in Alzheimer's disease

HONGBIN LIU[1], QINYUN LI[1], XIAODAN ZHANG[1], YUN SHI[1] and JINYI LI[2]

[1]No. 2 Department of Geriatrics, Beijing Geriatric Hospital, Beijing 100095;
[2]Dolu Health Consultant Co., Ltd., Tangshan, Hebei 063000, P.R. China

Received March 9, 2022; Accepted April 12, 2022

DOI: 10.3892/etm.2022.11353

Abstract. Alzheimer's disease (AD) is a progressive neurodegenerative dementia with the key pathological hallmark of amyloid deposits that may induce mitochondrial dysfunction. Ginkgolide K (GK) has been proven to have neuroprotective effects. The present study sought to explore the neuroprotective effect of GK through regulation of the expression of mitochondrial Ca^{2+} uniporter (MCU) in the pathology of AD. SH-SY5Y cells were cultured and the expression of MCU was enhanced by transfection of MCU recombinant vectors or knockdown by MCU small interfering RNA. The cells were treated with GK and amyloid β (Aβ). Thereafter, the effects of GK, MCU expression and Aβ on viability and apoptosis of SH-SY5Y cells were examined via a WST-1 assay, flow cytometry and Caspase-3/8 activity assays, respectively. The effects of GK, MCU expression and Aβ on the calcium levels in mitochondria were also examined. The regulatory effect of GK on MCU expression was examined by reverse transcription-quantitative PCR and western blot analysis. Furthermore, APP/PS1 mice received supplementation with GK and their cognitive ability was then examined through water maze tests, while the expression of MCU was examined using immunohistochemistry. The results indicated that enhancing the expression of MCU inhibited cell viability and promoted apoptosis. GK protected cells from amyloid-induced cytotoxicity by promoting cell viability and preventing cell apoptosis. The neuroprotective effect of GK was abolished when MCU expression was knocked down. GK decreased the expression of MCU *in vitro* and downregulation of MCU decreased the calcium level in mitochondria. Treatment with GK in APP/PS1 mice downregulated the expression of MCU in the brains and alleviated cognitive impairment. In conclusion, the present study demonstrated that the administration of GK protected neurons by preventing apoptosis. Furthermore, the neuroprotective effect of GK in neuronal cells was indicated to be related to the inhibition of MCU expression. Therefore, administration of GK may be a promising strategy for treating AD.

Correspondence to: Dr Hongbin Liu, No. 2 Department of Geriatrics, Beijing Geriatric Hospital, 118 Wenquan Road, Beijing 100095, P.R. China
E-mail: honbin1105@163.com

Dr Jinyi Li, Dolu Health Consultant, 62 Wenhua Road, Tangshan, Hebei 063000, P.R. China
E-mail: jinyili729@gmail.com

Key words: Alzheimer's disease, ginkgolide K, mitochondrial calcium uniporter

Introduction

Alzheimer's disease (AD) is one of the most common neurodegenerative diseases, with an estimated global prevalence of 6.2 million (1). AD has multiple clinical symptoms, including memory loss, confusion regarding time or place, decline in the ability to make decisions and judgments, aphasia, apraxia and agnosia, in addition to other symptoms, including fatigue, sleep disturbance, anxiety, depression and gastrointestinal dysfunction. Based on the knowledge acquired in recent years, various genomic factors, such as the presenilin 1 gene, amyloid-β (Aβ) precursor protein (APP) gene and apolipoprotein E gene, as well as certain epigenetic factors, contribute to the occurrence and progression of AD (2-4). A major pathological hallmark of AD is the presence of Aβ plaques. Aβ is generated from the Aβ precursor protein encoded by the APP gene, which is widely expressed in the central nervous system. Aβ peptides cause neurotoxicity in the brain by disrupting synaptic plasticity and promoting the production of nitric oxide formation. Furthermore, Aβ induces an influx of calcium ions (Ca^{2+}), which may then cause neuronal apoptosis. In fact, mitochondria mainly regulate cellular Ca^{2+} homeostasis via the expression of mitochondrial Ca^{2+} uniporter (MCU) to maintain neuronal survival and function (5,6). Conversely, dysregulation of MCU induces mitochondrial malfunction, contributing to neuronal apoptosis (6,7). Furthermore, mitochondrial dysfunction is another key factor involved in the pathogenesis of AD (8). Fu *et al* (9) discovered mitochondrial dysfunction in an AD mouse model. Taken together, these findings demonstrate that both Aβ and mitochondria have key roles in the pathogenesis of AD.

Ginkgolides are natural products isolated from *Ginkgo biloba* leaves. Ginkgolide K (GK) is a ginkgolide and a diterpene lactone compound. Multiple pharmacological properties of GK have been reported in previous studies, including neuroprotection (10), regulation of inflammation (11), antioxidative

stress (12) and potential benefits against ischemic stroke (13). In particular, Ma observed that GK treatment markedly protected PC12 cells against H_2O_2-induced cytotoxicity by ameliorating oxidative stress and mitochondrial dysfunction (14).

In the present study, the potential neuroprotective effect of GK on neuronal cell survival in AD pathology was explored. The results suggested that GK treatment decreased MCU expression, which contributes to the maintenance of calcium homeostasis and benefits neuronal cell survival (Fig. S1). Furthermore, GK supplementation regulated MCU expression in the brains of AD model mice and improved their cognitive ability.

Materials and methods

Cell culture. The human brain neuroblast cell line SH-SY5Y (CRL-2266) and the human cell line 293T (CRL-3216) were purchased from the American Type Culture Collection and were maintained in Eagle's minimum essential medium (Invitrogen; Thermo Fisher Scientific, Inc.) or Dulbecco's Modified Eagle's Medium (DMEM, HyClone; Cytiva), both of which were supplemented with 10% ultracentrifuged fetal bovine serum (FBS), penicillin (100 U/ml) and streptomycin (10 mg/ml; all from Invitrogen; Thermo Fisher Scientific, Inc.) at 37˚C in a humidified atmosphere with 5% CO_2. SH-SY5Y and 293T cells were seeded in a 96-well plate at 5,000 cells per well and maintained overnight for attachment. Thereafter, the cells were subjected to the different treatments for 72 h.

$A\beta_{25-35}$ was purchased from MilliporeSigma and diluted in DMSO for use at a concentration of 25 μm (15,16), while cells were treated with GK at a concentration of 50 μg/ml (12).

Transfection. SH-SY5Y cells were seeded into the wells of a 12-well plate at 10^5 cells per well and cultured at 37˚C with 5% CO_2. The cells were then transfected with small interfering (si)RNA against MCU (5'-GGAAAGGGAGCU UAUUGAA-3') or negative control siRNA (5'-UUCUCCGAA CGUGUCACGU-3') from Sangon Biotech at a final concentration of 40 nM using Lipofectamine® 2000 (Invitrogen; Thermo Fisher Scientific, Inc.) following the manufacturer's protocol. The transfection efficiency was validated by reverse transcription-quantitative (RT-q)PCR or western blot analysis. At 24 h post-transfection, cells were used for the subsequent experiments.

Plasmid construction and transfection. The protein-coding sequences of human MCU cDNAs (sequence proofed, OriGene Technologies, Inc.) was subcloned into the pcDNA3.1 expression vector (Thermo Fisher Scientific, Inc.). The expression vector and 4 μg lentiviral vector (MilliporeSigma) were then transfected into 293T cells using the calcium phosphate precipitation method for 48 h following the manufacturer's protocol. Subsequently, the culture medium of 293T cells was replaced with DMEM supplemented with 5% FBS, followed by incubation for 48 h. The viral supernatant was then collected, centrifuged at 250 x g for 5 min at 4˚C and passed through a filter membrane (pore size, 0.45 μm; EMD Millipore). SH-SY5Y cells were incubated at 37˚C with the recombinant lentiviral vectors at a multiplicity of infection of 30 using the FuGENE Transfection Reagent (Roche Diagnostics) and were used for further experiments after 72 h. Western blot analysis was performed to verify the interference efficiency.

Western blot analysis. Total protein was collected from the cells using RIPA buffer (MilliporeSigma) containing protease inhibitors and the protein concentrations were determined by the BCA method. Equal amounts of protein (20 μg/lane) were loaded and separated on SDS-polyacrylamide gels (8-10%) for electrophoresis. Thereafter, the protein bands on the gels were transferred to nitrocellulose membranes (MilliporeSigma). The membranes were then blocked with 5% bovine serum albumin (diluted in Tris-Cl-buffered saline with 0.1% Tween-20) for 2 h at room temperature and incubated with primary antibodies at 1:3,000 dilution overnight at 4˚C. Subsequently, the membrane was incubated with secondary antibodies (1:3,000 dilution; anti-mouse IgG or anti-rabbit IgG; cat. nos. ab205719 and ab205718; Abcam). The blot was then detected using the Western Bright ECL western blotting detection kit (Bio-Rad Laboratories, Inc.). Equal sample loading was verified by detection of GAPDH. The primary antibodies were as follows: Mouse monoclonal anti-GAPDH (cat. no. sc-32233; Santa Cruz Biotechnology, Inc.), rabbit monoclonal anti-MCU (cat. no. ab272488; Abcam), rabbit polyclonal anti-Aβ (cat. no. 51-2700; Invitrogen; Thermo Fisher Scientific, Inc.), mouse monoclonal anti-tau (cat. no. sc-390476; Santa Cruz Biotechnology, Inc.) and rabbit monoclonal anti-tau (phospho Ser214; cat. no. ab170892; Abcam).

RNA isolation and RT-qPCR. Total RNA was extracted from the cells using the RNeasy kit (Qiagen GmnH) following the manufacturer's protocol and then reverse-transcribed into cDNA using SuperScript™ III Reverse Transcriptase (Invitrogen; Thermo Fisher Scientific, Inc.). mRNA expression was measured using an ABI PRISM 7500 Real-Time qPCR System according to the manufacturer's protocol. Candidate gene expression was measured using a SYBR Green-based reagent (SYBR GreenER qPCR SuperMix for iCycler; Invitrogen; Thermo Fisher Scientific, Inc.) and a real-time qPCR system (ABI PRISM 7500 Real-Time PCR System; Thermo Fisher Scientific, Inc). The cycling conditions for the reaction were as follows: 10 min at 95˚C for initial hold; then 40 cycles of 15 sec at 95˚C for denaturation, 30 sec at 60˚C for annealing and a 30 sec extension at 72˚C. The following primers were used: MCU forward, 5'-ACCGGACGGTAC ACCAGAG-3' and reverse, 5'-GATAGGCTTGAGTGTGAA CTGAC-3'; and GAPDH forward, 5'-TGTGGGCATCAA TGGATTTGG-3' and reverse, 5'-ACACCATGTATTCCG GGTCAAT-3'. All PCR analyses were performed in triplicate and expression values were quantified with the corresponding standard curves. The expression of MCU was normalized to GAPDH expression. Relative quantitation of gene expression was performed using the $2^{-\Delta\Delta Cq}$ method (17).

Cell viability assay. SH-SY5Y cells with various transfections were seeded into 96-well plates (5,000 cells/well) and maintained overnight for attachment. The cells were then treated with Aβ, GK or Aβ+GK respectively and further cultured for 72 h. Subsequently, cell viability was measured via the WST-1 assay (Roche Diagnostics) according to the manufacturer's protocol. The absorbance was read at 440 nm using a

Multimode Plate Reader (Varioskan™ LUX; Thermo Fisher Scientific, Inc.).

Apoptosis assay. Following cell treatment as specified above, flow cytometry was applied to evaluate the apoptosis of SH-SY5Y cells *in vitro*. After 72 h of treatment, the cells were collected, washed with PBS and resuspended in 100 μl binding buffer at a concentration of 10^6 cells/ml. Subsequently, 5 μl annexin V-FITC and 10 μl propidium iodide (both purchased from Beyotime Institute of Biotechnology) were added to the cell suspension, which was then incubated for 15 min at room temperature in the dark. Finally, the rate of apoptosis in each cell sample was examined using a FACScan flow cytometer (BD Biosciences) and the data were analyzed by FlowJo software (V10.6; BD Biosciences).

Caspase-3/8 activity. The Caspase-3 (cat. no. C1168S) and Caspase-8 (cat. no. C1152) kits were both purchased from Beyotime Institute of Biotechnology and used to measure the respective activities of Caspase-3/8 following the manufacturer's protocols. The cells were collected after the treatments and total protein was extracted from the cells using lysis buffer, and then mixed with 85 μl reaction buffer. Subsequently, 5 μl Leu-Glu-His-Asp-p-nitroanilide was added to the protein samples, followed by incubation at 37˚C for 2 h. A multiplate reader (Varioskan™ LUX; Thermo Fisher Scientific, Inc.) was used to measure the activities of Caspase-3/8 at 450 nm.

Ca^{2+} uptake assay. The mitochondria were isolated by using a mitochondria isolation kit for Cultured Cells (cat. no. 89874; Thermo Fisher Scientific, Inc.) and then dissolved in swelling buffer provided with the kit. The protein concentration of the mitochondria solution was determined by the BCA method at 5 mg/ml. After 30 min of application of $CaCl_2$ (100 μM) to the solution, the mitochondria were collected by centrifugation (3,000 x g) for 15 min at 4˚C. The pellets were resuspended in swelling buffer containing 1 μM ruthenium red. After collecting the mitochondria through centrifugation (3,000 x g) for 15 min at 4˚C, the pellets were dried and dissolved in 40 μl 0.75 M sulfuric acid at 95˚C. The solution was then diluted with water and the Ca^{2+} concentration of the solution was measured by an atomic absorbance spectrometer (iCE™ 3300 AAS; Thermo Scientific, Inc.).

APP/PS1 mice. The procedures and experiments in this study were approved by the Committee on Ethics of Animal Experiments, Beijing Geriatric Hospital (no. 2019134). All animal care procedures and experiments were conducted in accordance with the Animal Research: Reporting of *In Vivo* Experiments guidelines (18). The APP/PS1 mice (n=20 in total) were purchased from The Jackson Laboratory and were used in all experimental groups (n=10 mice/group; male-to-female ratio, 1:1; body weight, 21.43±2.42 g). Mice were housed in the Experimental Animal Facility (five mice per cage) of Beijing Geriatric Hospital (Beijing, China) under standard laboratory conditions (18-23˚C; 40-60% humidity; 12-h light/dark cycle) with free access to food and water. Animal health and behavior were monitored every 2 days.

GK was purchased from Shanghai Bohu Biotechnology and dissolved in DMSO. GK was administered intraperitoneally at 8 mg/kg (10), while the control mice were treated with DMSO. In total, 20 mice (age, 6 months) were used in the experiments. The mice received GK treatment or DMSO for 1 month before they were subjected to the water maze test (19). Thereafter, the mice were euthanized via carbon dioxide inhalation (replacement of 50% of the chamber volume/min). Death of the mice was confirmed by lack of a heartbeat, lack of respiration, lack of corneal reflex and presence of rigor mortis.

During the water maze test, distress was monitored by observing animal behavior. The water was warmed to room temperature before the mice are placed in it. In the maze test, mice were placed gently in the water hindfeet-first to avoid stress. The mice that were agitated or became unable to swim were rescued immediately. Overtiring or hypothermia of mice were prevented by limiting the swimming duration. Mice were dried upon completion of the task before their return to their home cage. In addition, the water was changed daily to prevent growth of pathogenic organisms (20).

Morris water maze test. The spatial learning ability and memory of mice were assessed using the Morris water maze test by measuring the latency to find a hidden platform submerged in a pool (21). The training protocol was applied for five consecutive days, with four trials per day in a water maze. In each trial, the mice were placed into the water at a different starting point and were allowed to swim and find the hidden platform within 90 sec. The mice that failed to find the platform were guided to the platform manually and kept at the platform for 10 sec. Thereafter, on day six, the platform was removed from the pool and the spatial probe test was conducted. Each mouse was placed in the water in a location opposite the target quadrant, facing the wall of the pool. The time that the mice spent in the target quadrant was recorded over a period of 90 sec. A tracking camera device (Ethovision 2.0; Noldus) was used to monitor the behavioral experiments and the recording was analyzed using video-tracking software (DigBehv Animal Behavior Analysis Software 1.0; Shanghai Jiliang Software Technology Co., Ltd.).

Immunohistochemistry (IHC). Brain tissues were fixed with 10% formalin for 24 h at room temperature and embedded in paraffin. Paraffin-embedded tissue samples were then cut into 5-μm-thick sections. The sections on glass slides were deparaffinized with xylene at 55˚C, rehydrated with a descending alcohol series and then subjected to antigen retrieval. Next, the sections were blocked with 5% goat serum (Thermo Fisher Scientific, Inc.) at room temperature for 1 h. The sections were then stained with antibody (1:200 dilution) against MCU (cat. no. PA5-120437; Invitrogen; Thermo Fisher Scientific, Inc.) or Aβ (cat. no. 51-2700; rabbit polyclonal; Invitrogen; Thermo Fisher Scientific, Inc.) and incubated with a horseradish peroxidase-labeled dextran polymer coupled with an anti-rabbit antibody (1:1,000 dilution; Beyotime Institute of Biotechnology) at room temperature for 1 h. Staining that was clearly distinguishable from the background was considered positive. The staining results were visualized using a light microscope (Olympus Corporation). The expression level of MCU was quantified by the optical density values in 10 random area fields under a magnification of x400 according to the regular IHC staining grade system (22). The load of Aβ

was quantified as the percentage area of Aβ deposits within the image cubes made with a multispectral imaging system (23).

Statistical analysis. Values are expressed as the mean ± standard error of the mean. SPSS 26 software (IBM Corporation) was used to analyze the data. An unpaired independent Student's t-test or one-way ANOVA followed by Tukey's post-hoc test were used to compare multiple groups. $P<0.05$ was considered to indicate a statistically significant difference.

Results

Regulatory effect of MCU on the viability and apoptosis of SH-SY5Y cells. To investigate the effect of MCU in SH-SY5Y cells, the expression of MCU was enhanced by transfection of recombinant lentiviral vectors or by blocking the expression of MCU with siRNA (Fig. 1A).

In the cell viability assay, it was observed that ectopic expression of MCU by transfection inhibited cell viability, while knockdown of the expression of MCU by siRNA increased cell viability (Fig. 1B). Furthermore, the cells were collected after different treatments, stained with annexin V and PI and analyzed using flow cytometry to evaluate apoptosis. The results indicated that MCU expression enhancement by transfection promoted the percentage of apoptotic SH-SY5Y cells, whereas blocking the expression of MCU significantly decreased the apoptotic rate of SH-SY5Y cells (Fig. 1C). In addition, Caspase-3/8 activities were examined in the cells. Consistently, overexpression of MCU increased the activities of both Caspase-3 and Caspase-8; by contrast, blocking the expression of MCU decreased the activities of both Caspase-3 and Caspase-8 (Fig. 1D).

Effect of GK on the viability and apoptosis of SH-SY5Y cells. It is known that Aβ is able to induce apoptosis in neuronal cells and contribute to AD pathology in mammals. In the present study, Aβ was used to treat SH-SY5Y cells and the results indicated that Aβ treatment inhibited cell viability (Fig. 2A). Furthermore, cotreatment with GK alleviated the cytotoxicity caused by Aβ. The cells cotreated with GK had a higher viability rate than the cells without GK treatment (Fig. 2A). The cell viability exhibited a significant difference when the cells were treated with GK alone compared to the control group (treatment with DMSO). In addition, Aβ treatment increased the cell apoptosis rate, whereas the administration of GK significantly attenuated Aβ-induced apoptosis in SH-SY5Y cells with a decrease in the apoptosis rate and Caspase-3/8 activities (Fig. 2B and C).

The present results indicated that GK failed to promote cell viability and inhibit apoptosis when MCU expression was knocked down. When MCU expression was knocked down, there were no significant differences in cell viability (Fig. 3A), apoptosis rate (Fig. 3B) or Caspase-3/8 activities (Fig. 3C) between the Aβ+GK treatment group and the GK treatment group.

GK regulates Ca^{2+} levels through MCU expression in mitochondria. The potential interaction between GK and MCU was then investigated. The present results indicated that Aβ significantly increased the expression of MCU, while GK decreased the expression of MCU at both the mRNA and protein levels (Fig. 4). Furthermore, in SH-SY5Y cells, the promoting effect of Aβ on MCU expression was clearly inhibited by cotreatment with GK. In addition, treatment with GK did not affect the expression levels on Aβ, tau protein and phosphorylated-tau protein (Fig. S2).

To investigate the effect of MCU on the Ca^{2+} levels in mitochondria, MCU expression was knocked down in cells using siRNA (Fig. 1). It was observed that a deficit in MCU expression decreased the level of Ca^{2+} in the mitochondria of SH-SY5Y cells (Fig. 5). Furthermore, treatment with GK reduced the levels of Ca^{2+} in the mitochondria of SH-SY5Y cells. The inhibitory effect of GK on the levels of Ca^{2+} in the mitochondria of SH-SY5Y cells was alleviated by blocking MCU (Fig. 5). No significant difference was observed in Ca^{2+} levels in mitochondria between the MCU knockdown cells with and those without GK treatment.

Thus, the present results suggested that GK was able to regulate MCU expression and then reduce the levels of Ca^{2+} in the mitochondria of the cells.

Administration of GK decreases the levels of MCU and Aβ deposits and improves cognitive ability in APP/PS1 mice. APP/PS1 mice (age, 6 months) received GK for 1 month. Thereafter, the Morris water maze test was used to assess spatial learning and cognitive ability. In the mice with GK supplementation, the latency to find the hidden platform was significantly decreased compared with that of the control mice, and the performance of the mice with GK supplementation was significantly improved in terms of the numbers of platform crossings (Fig. 6). Furthermore, mouse cortex tissues were collected and IHC staining for MCU in brain sections revealed strong MCU expression in the cortex. IHC analysis also indicated that GK supplementation decreased the expression level of MCU protein (Fig. 7A).

In addition, IHC staining against Aβ identified extracellular Aβ-positive deposits and intracellular granules in the neuronal cell body in the brain cortex. The deposits were dense and spherical. Qualitative assessment of Aβ deposition did not indicate any obvious difference in the number of Aβ plaques in mice with/without GK administration (Fig. 7B).

Discussion

In the present study, the effect of GK on AD pathology was examined and the underlying mechanisms were investigated. It was revealed that GK was able to promote cell viability and prevent apoptosis induced by Aβ by regulating the expression of MCU *in vitro*. In line with this, GK treatment decreased the expression of MCU in the mouse brain and alleviated the impairment in the cognitive ability of APP/PS1 mice.

In the brain, the amyloid precursor protein is cleaved by β-site amyloid precursor protein-cleaving enzyme 1 to generate Aβ. Increased Aβ activity has consistently been detected in the brain tissue of patients with AD and has a key role in the occurrence and progression of AD (24). It was observed that treatment with Aβ resulted in neuronal cell apoptosis. Aβ may exert its neurotoxic effects via multiple pathways. Aβ contributes to the generation of lipid peroxides and carbonyls, which

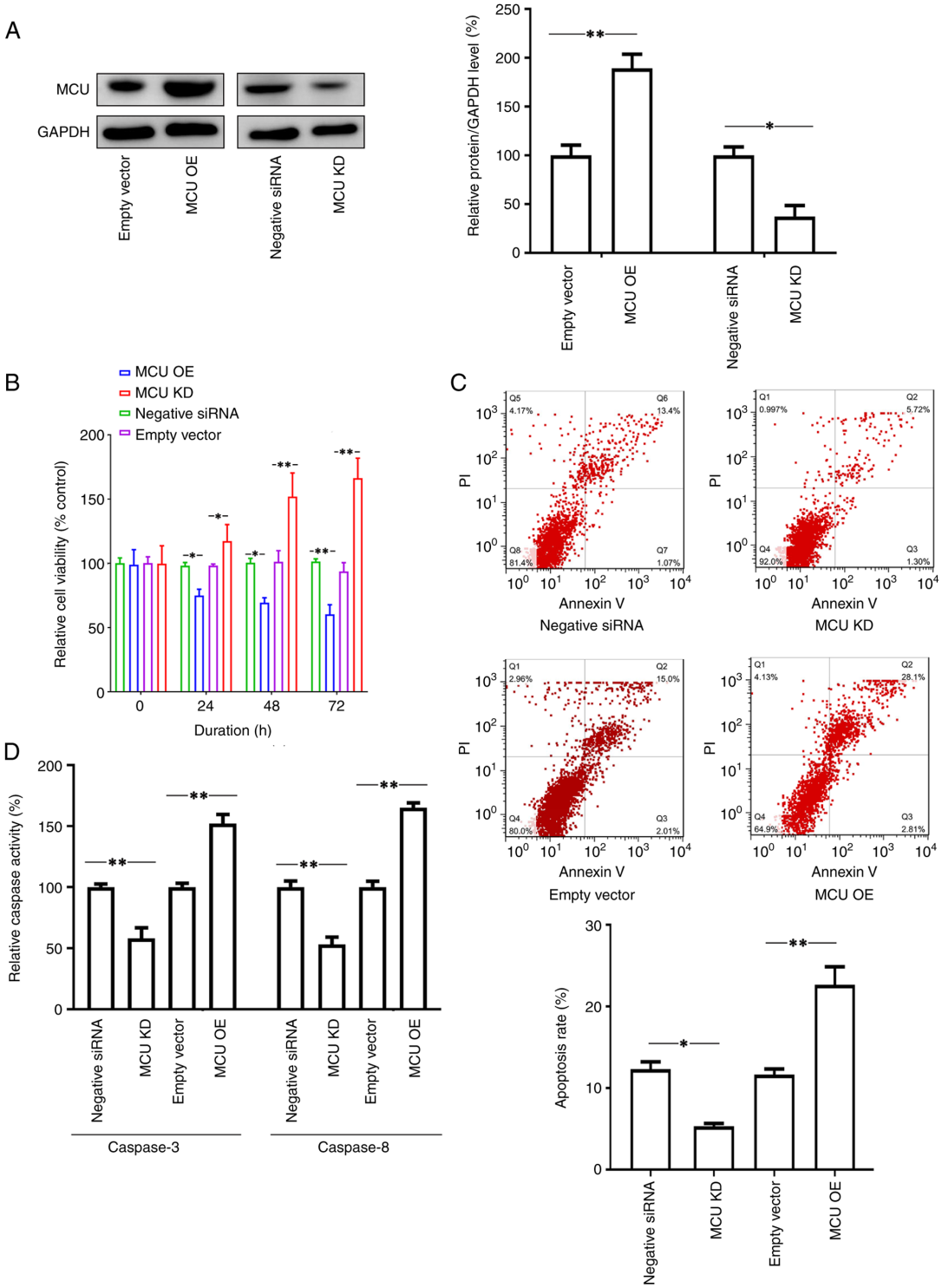

Figure 1. Effects of MCU on the viability and apoptosis of SH-SY5Y cells. SH-SY5Y cells were cultured *in vitro* and then transfected with recombinant lentiviral vectors to overexpress MCU or knockdown expression MCU by transfection of MCU siRNA, while cells transfected with empty vector or negative control siRNA were used as controls. Thereafter, the cells were cultured for 72 h and cell viability, apoptosis and Caspase-3/8 activities were examined. (A) Transfection of recombinant lentiviral vectors (MCU OE) increased MCU expression compared to the transfection of empty vector, while knockdown of MCU by transfection of siRNA (MCU KD) inhibited MCU expression compared to the transfection of negative control siRNA. Representative images of the western blot analysis and quantified results are provided. (B) Knockdown of MCU promoted cell viability. The cells with different pretreatments (MCU OE or MCU KD) were cultured *in vitro* for 72 h and cell viability was measured by a WST-1 assay. The results indicated that the cells with MCU expression enhancement had lower cell viability rates compared to the controls (empty vector transfection), whereas knockdown of MCU increased cell viability compared to that in cells transfected with negative siRNA. (C) Apoptotic cells were measured by FACScan after staining with annexin V and PI. The sum of annexin V-positive cells and annexin V- + PI-positive cells was used to indicate the total percentage of apoptotic cells. The expression enhancement of MCU promoted apoptosis in SH-SY5Y cells, which was significantly higher than that in the control group. However, blocking the expression of MCU decreased the rate of apoptosis of the cells. Representative images and relative quantifications are presented. (D) The data on apoptotic protein activities (Caspase-3 and Caspase-8) were consistent with the results of flow cytometry. Expression enhancement of MCU promoted the activity of Caspase-3 and Caspase-8 in cells. Blocking the expression of MCU resulted in lower activity of Caspase-3 and Caspase-8 in cells. All results are representative of three independent experiments performed in triplicate. Values are expressed as the mean ± standard error of the mean. *P<0.05; **P<0.01, one-way ANOVA followed by Tukey's post-hoc test. siRNA, small interfering RNA; KD, knockdown; OE, overexpression; PI, propidium iodide; Q, quadrant; MCU, mitochondrial Ca^{2+} uniporter.

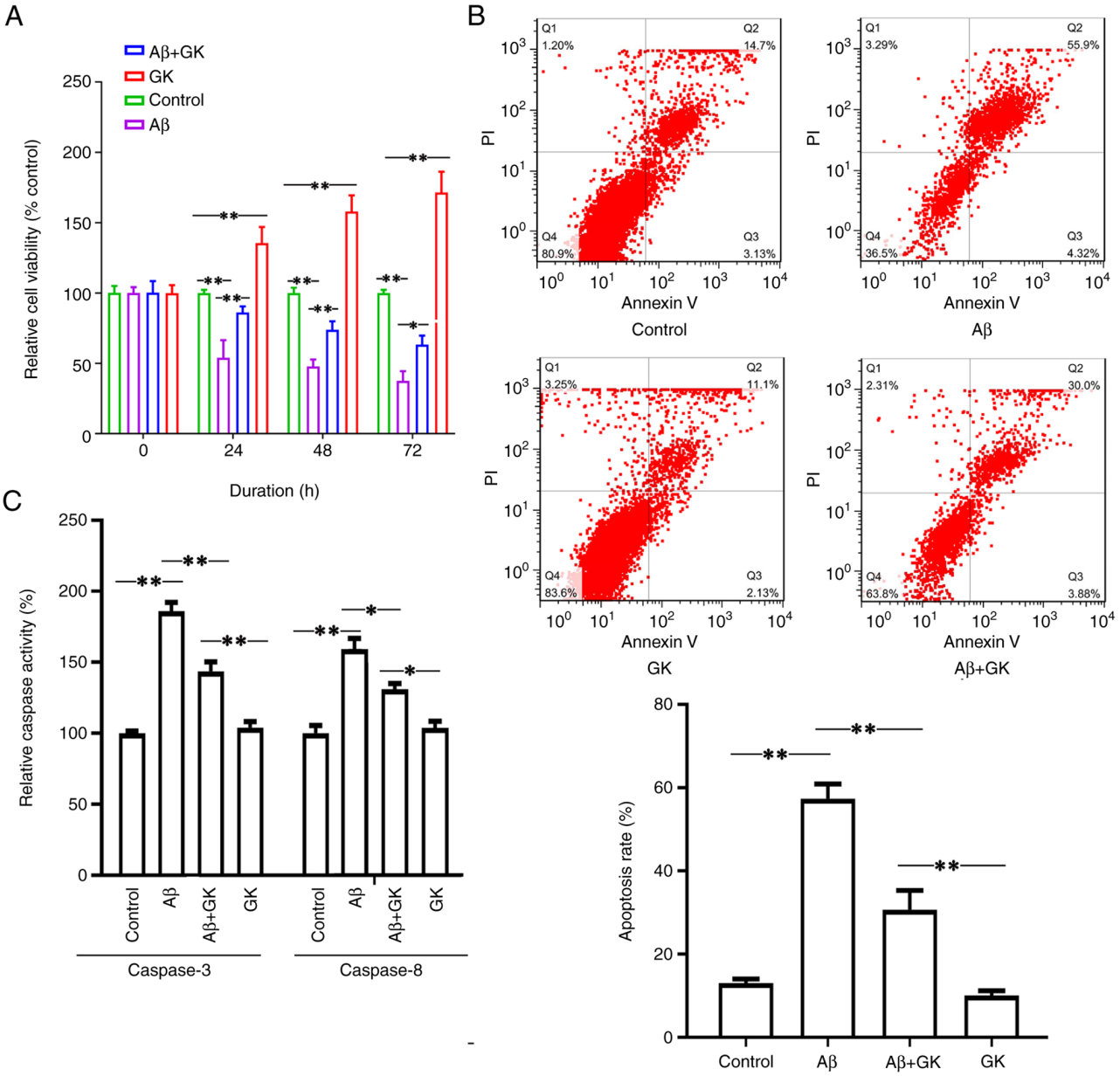

Figure 2. Treatment with GK promotes cell viability and prevents apoptosis of SH-SY5Y cells *in vitro*. SH-SY5Y cells were cultured *in vitro* and then treated with GK (50 μg/ml), Aβ (25 μM) or GK (50 μg/ml)+Aβ (25 μM) for 72 h, while cells treated with DMSO were used as controls. (A) Cell viability was measured using WST-1. The results indicated that Aβ treatment inhibited cell viability compared to the controls, whereas cotreatment with GK alleviated the inhibitory effect of Aβ on SH-SY5Y cell viability. Treatment with GK promoted cell viability compared to the controls. (B and C) Apoptotic cells were measured by FACScan after staining with annexin V and PI. (B) The sum of annexin V-positive cells and annexin V- + PI-positive cells was used to indicate the total percentage of apoptotic cells. (C) The activities of Caspase-3 and Caspase-8 were also measured as described in the methods. Aβ treatment promoted cell apoptosis rates and increased the activities of Caspase-3 and Caspase-8 compared to the controls, whereas cotreatment with GK alleviated the proapoptotic effect of Aβ on SH-SY5Y. All experiments were performed in triplicate. Values are expressed as the mean ± standard error of the mean. *P<0.05; **P<0.01, one-way ANOVA followed by Tukey's post-hoc test. PI, propidium iodide; Q, quadrant; GK, ginkgolide K; Aβ, amyloid β.

then induce damage to neuronal cells (25). Furthermore, it has been indicated that the toxic properties of Aβ are mediated by several other mechanisms, including inflammation, synaptic dysfunction and excitotoxicity (26).

Another potential mechanism of the effect of Aβ on AD pathology may be through Ca^{2+} regulation of neuronal cells. Aβ may cause the formation of Ca^{2+}-permeable pores in artificial membranes (27) and then regulate Ca^{2+} entry into the cytoplasm of brain cells (28). Furthermore, Ca^{2+} homeostasis in mitochondria maintains regular neuronal function (8). In the present study, it was observed that increased Ca^{2+} levels in mitochondria resulted in a higher apoptosis rate of neuronal cells. In fact, the loss of Ca^{2+} homeostasis in the mitochondria of neuronal cells of patients with AD has been observed by previous studies (29,30). Mitochondrial dysfunction is another factor in AD pathogenesis that is involved in cell survival and synaptic plasticity (31). Perez *et al* (32) reported mitochondrial Ca^{2+} dysregulation in the fibroblasts of patients with AD. Calvo-Rodriguez *et al* (33) observed elevated Ca^{2+} levels in neuronal mitochondria after significant Aβ plaque deposition in an AD mouse model. In the present study, it was observed that treatment with Aβ resulted in apoptosis of neuronal cells,

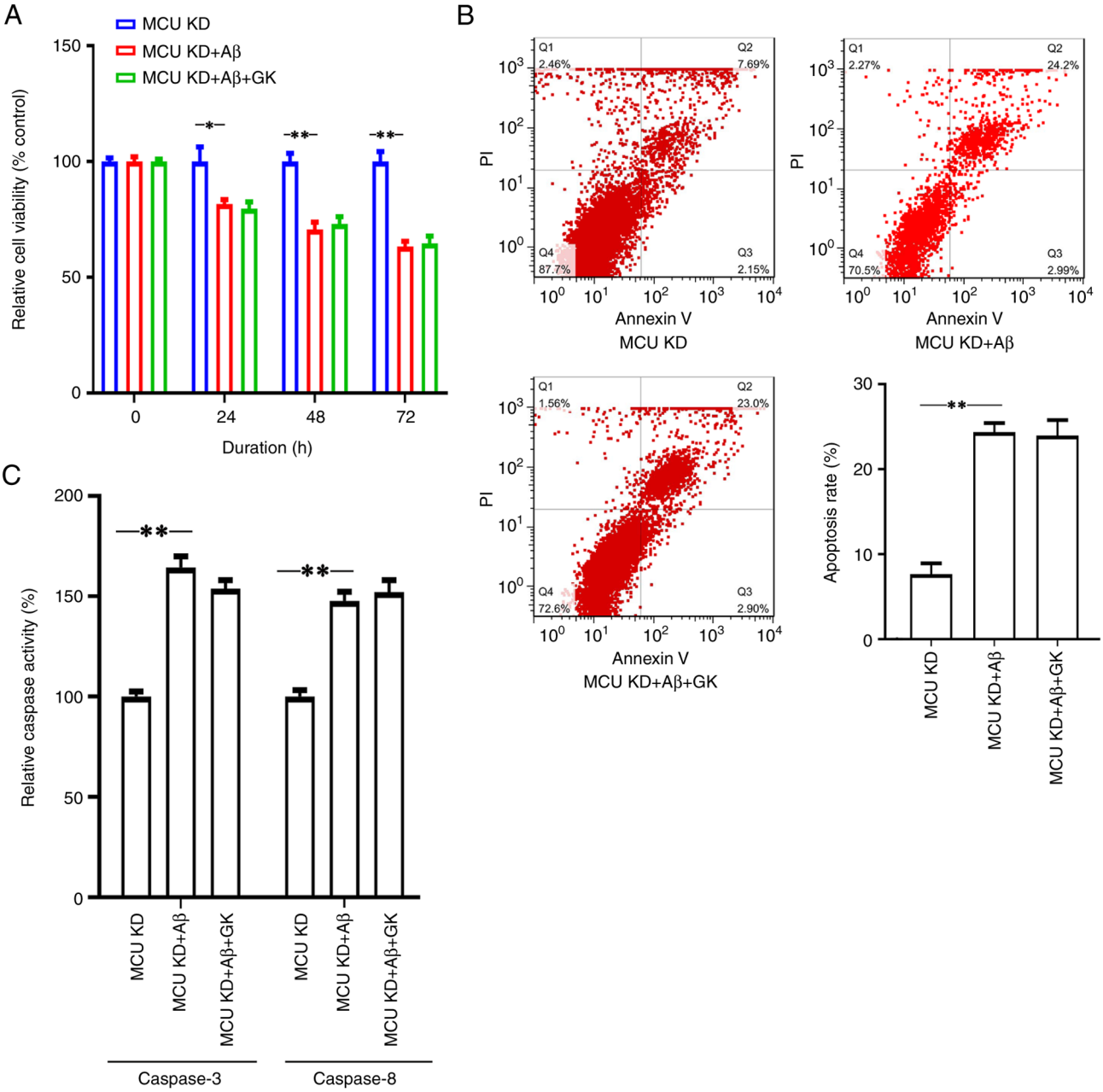

Figure 3. Knocking down the expression of MCU alleviates the promotion effect of GK on SH-SY5Y cells in the presence of Aβ. SH-SY5Y cells were cultured *in vitro* and the expression of MCU was knocked down by siRNA transfection. The cells were then treated with Aβ (25 μM) or GK (50 μg/ml)+Aβ (25 μM) for 72 h, while cells treated with DMSO were used as controls. Cell viability was measured using WST-1. Apoptotic cells were measured by FACScan after staining with annexin V and PI. The sum of annexin V-positive cells and annexin V- + PI-positive cells was used to indicate the total percentage of apoptotic cells. Treatment with Aβ (A) decreased cell viability, (B) promoted cell apoptosis and (C) increased the activities of Caspase-3 and Caspase-8 compared to the control (DMSO). However, cotreatment with GK failed to alleviate (A) the inhibitory effect on cell viability or (B and C) the promotion effect on cell apoptosis by Aβ in SH-SY5Y cells with MCU knocked down in terms of (B) the apoptotic rate measured by flow cytometry and (C) caspase activity. All experiments were performed in triplicate. Values are expressed as the mean ± standard error of the mean. *P<0.05; **P<0.01 by one-way ANOVA followed by Tukey's post-hoc test. MCU, mitochondrial Ca^{2+} uniporter; PI, propidium iodide; Q, quadrant; GK, ginkgolide K; Aβ, amyloid β; siRNA, small interfering RNA; KD, knockdown; OE, overexpression.

as well as increased Ca^{2+} levels in mitochondria, which may explain the potential interaction between Aβ deposits and mitochondrial Ca^{2+} dyshomeostasis in AD pathology. Aβ is able to increase mitochondrial Ca^{2+} levels and result in neuronal death in an AD mouse model, which has been observed in multiple studies (33-35). Aβ is also able to promote excessive Ca^{2+} release from the endoplasmic reticulum to mitochondria and induce mitochondrial Ca^{2+} overload, triggering neuronal cell death (36). By contrast, decreasing the mitochondrial Ca^{2+} levels with the MCU blocker RU360 alleviated the impact on cognitive ability in an AD rat model (37).

The potential protective effect of GK in neuronal cells has been previously reported. Liu *et al* (12) indicated that GK protected SH-SY5Y cells against oxygen/glucose deprivation stress. The present study reported that treatment with GK promoted viability and prevented apoptosis of neuronal cells. Furthermore, GK exerted a prosurvival effect by regulating the function of mitochondria. Zhou *et al* (10) suggested that

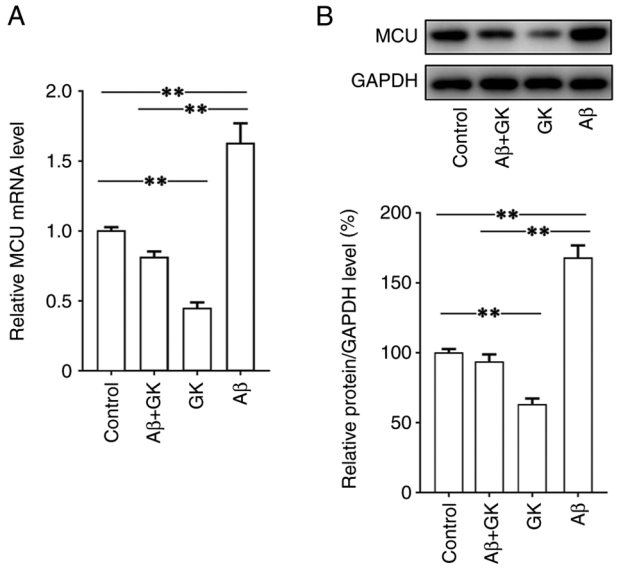

Figure 4. GK inhibits MCU protein in SH-SY5Y cells. SH-SY5Y cells were cultured *in vitro* and then treated with GK (50 μg/ml), Aβ (25 μM) or GK (50 μg/ml)+Aβ (25 μM) for 72 h, while cells treated with DMSO were used as controls. MCU expression was examined using both reverse transcription-quantitative PCR and western blot analysis. The results indicated that Aβ treatment increased MCU expression compared to the controls, whereas cotreatment with GK alleviated the promotion effect of Aβ on MCU expression at (A) the mRNA level and (B) protein level. Treatment with GK decreased MCU expression compared to the controls at the mRNA and protein levels. Values are expressed as the mean ± standard error of the mean derived from 3 independent experiments. **P<0.01 according to 2-tailed unpaired Student's t-test or one-way ANOVA followed by Tukey's post-hoc test. MCU, mitochondrial Ca^{2+} uniporter; GK, ginkgolide K; Aβ, amyloid β.

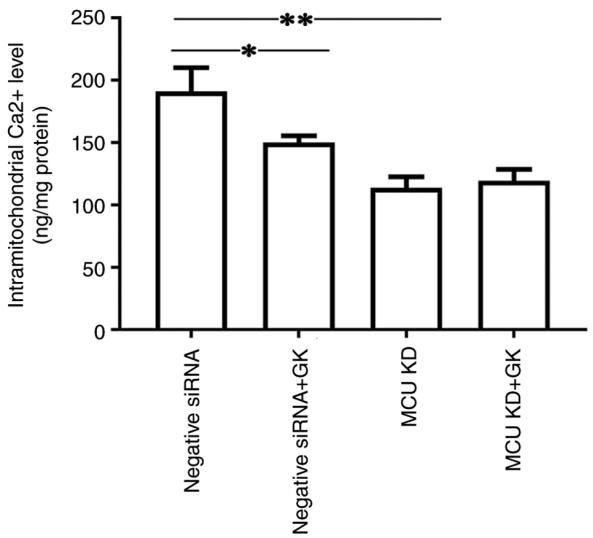

Figure 5. GK decreases Ca^{2+} levels in the mitochondria of SH-SY5Y cells. SH-SY5Y cells were cultured *in vitro* and the expression of MCU was knocked down by siRNA transfection, while cells transfected with negative control siRNA were used as controls. The cells were then treated with GK at 50 μg/ml or DMSO for 72 h. Thereafter, the Ca^{2+} levels in mitochondria were measured. GK decreased the Ca^{2+} level in the mitochondria of SH-SY5Y cells. Knockdown of MCU (MCU KD) in SH-SY5Y cells decreased the Ca^{2+} levels in the mitochondria. However, treatment with GK failed to regulate the Ca^{2+} levels in the mitochondria of SH-SY5Y cells when MCU expression was knocked down. Values are expressed as the mean ± standard error of the mean derived from 3 independent experiments. *P<0.05; **P<0.01 by one-way ANOVA followed by Tukey's post-hoc test. MCU, mitochondrial Ca^{2+} uniporter; GK, ginkgolide K; Aβ, amyloid β; siRNA, small interfering RNA; KD, knockdown.

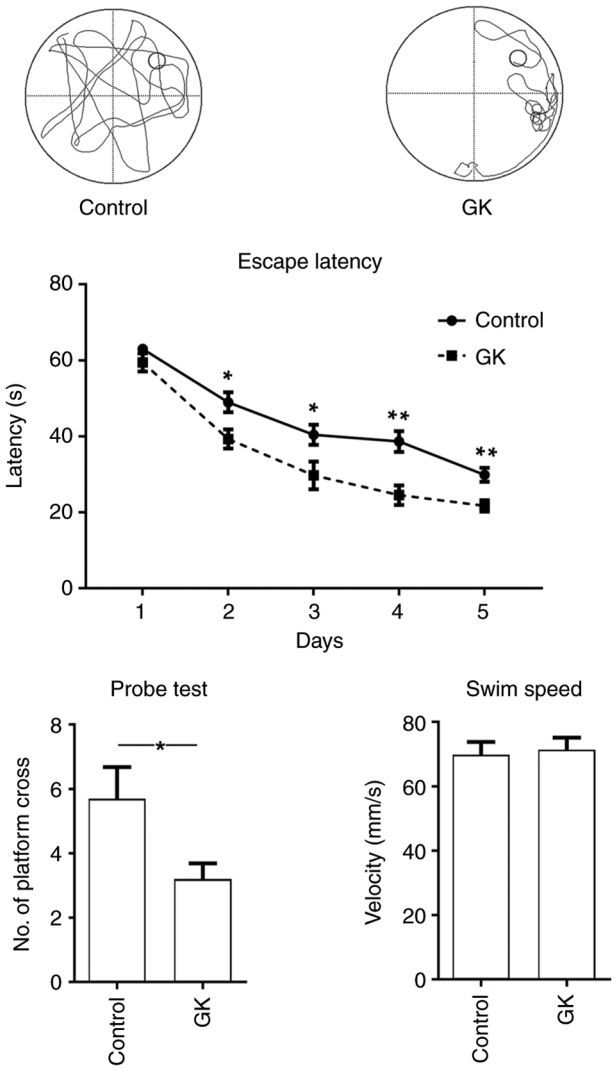

Figure 6. GK treatment improves the cognitive ability of APP/PS1 mice. APP/PS1 mice (age, 6 months; n=10 mice/group) received 8 mg/kg GK treatment intraperitoneally for 1 month, while mice treated with DMSO were used as controls. After the treatments, the mice were assessed in the Morris water maze. The mice were placed into the water at a different starting point each time and were allowed to swim and find the hidden platform within 90 sec for five consecutive days. On day six, the platform was removed from the pool and the spatial probe test was performed, in which the time that the mice spent in the target quadrant was recorded for a period of 90 sec. The average latency to find the hidden platform per day was assessed for each mouse in each group after the training period. GK supplementation significantly decreased the latency to find the platform compared to the control group. The number of target platform crossings during the probe trial was significantly increased in the GK supplementation group compared to the control group. The average swim velocity was calculated for each mouse and described as the average per group, with no significant difference between GK-supplemented mice and control mice. Values are expressed as the mean ± standard error of the mean. *P<0.05; **P<0.01 by 2-tailed unpaired Student's t-test. GK, ginkgolide K.

GK inhibits mitochondrial fission and membrane permeability, while Ma *et al* (14) suggested that GK contributes to maintaining the function of mitochondria. Similarly, in the present study, it was observed that GK inhibited the expression of MCU in neuronal cells. MCU is one of the most prominent calcium uniporters on the inner membrane of mitochondria. In cells, efficient mitochondrial uniporter-mediated Ca^{2+} uptake is required for MCU action. However, dysfunction of MCU

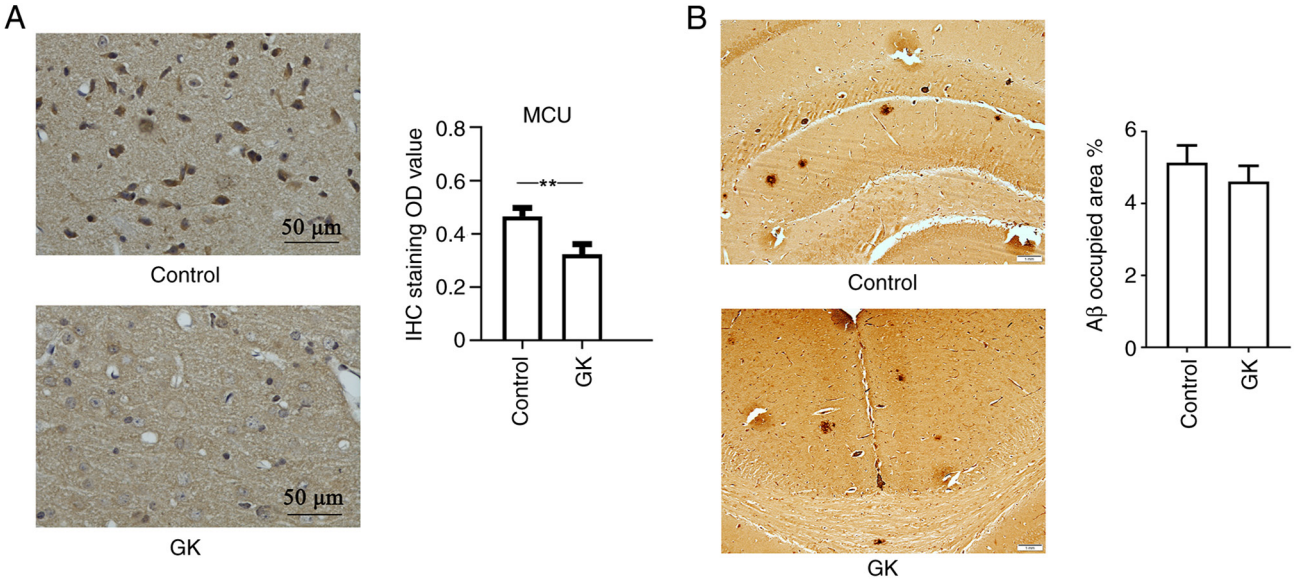

Figure 7. MCU expression and Aβ deposits in APP/PS1 mice with GK supplementation. APP/PS1 mice (age, 6 months old; n=10 mice/group; male-to-female ratio, 1:1) were administered 8 mg/kg GK intraperitoneally for 1 month, while mice treated with DMSO were used as controls. After the treatments, the mouse brains were collected and cut into sections. The sections were then stained with antibody against MCU. The staining results were visualized using a light microscope. (A) IHC staining of the cortex of mice indicated clear positive expression of MCU in neuronal cells. Quantitative data indicated that GK supplementation significantly inhibited the expression of MCU in the cerebral cortex of mice. The expression levels of MCU were semiquantified according to the standard IHC staining grade system (scale bar, 50 μm). (B) IHC staining of brain tissues was performed using antibodies against Aβ. Aβ load was estimated by stereology and presented as % positive staining of the image area. Qualitative assessment of Aβ deposition did not indicate any significant difference in the number of Aβ plaques between mice with and those without GK administration (scale bar, 1 mm). Values are expressed as the mean ± standard error of the mean. **P<0.01, by 2-tailed unpaired Student's t-test. MCU, mitochondrial Ca^{2+} uniporter; GK, ginkgolide K; IHC, immunohistochemistry; Aβ, amyloid β.

may lead to loss of Ca^{2+} homeostasis, promoting the influx of Ca^{2+} in the mitochondria. The present results indicated that blocking the expression of MCU decreased Ca^{2+} in the mitochondria. In AD pathology, increased activity of MCU may contribute to Ca^{2+} influx and excessive Ca^{2+} in mitochondria would then inhibit ATP production and trigger neuronal cell apoptosis and synapse dysfunction (38). The results of the present study suggested data that overexpression of MCU led to an increase in apoptosis and a decrease in viability of neuronal cells, whereas blocking the expression of MCU promoted the survival of neuronal cells with decreased apoptosis and increased viability. Furthermore, it was observed that Aβ treatment promoted the expression of MCU *in vitro*, which is consistent with previous studies (33,34,39). Thus, it may be suggested that the dysregulation of MCU in mitochondria induced by Aβ may be one of the pathological mechanisms of AD, while targeting the expression of MCU may contribute to the survival of neuronal cells in AD brains.

The neuroprotective effect of *Ginkgo biloba* has been demonstrated by previous studies (40-42). The mechanism of action of *Ginkgo biloba* may proceed through multiple pathways, including antioxidative stress, regulation function of mitochondria and anti-inflammation (40-42). However, *Ginkgo biloba* contains numerous types of chemical components, such as terpenoids, biflavones and flavonols (42). Furthermore, among the active ingredients of *Ginkgo biloba*, terpenoids include the main diterpene ginkgolides A, B, C, J, M, K and L (43). Different active components may exert their functions through the regulation of different pathways. Although the regulation of mitochondria by *Ginkgo biloba* extracts has been revealed, there is a lack of knowledge regarding which type of monomer contributes to the maintenance of mitochondrial function. Thus, research on the monomers of *Ginkgo biloba* extracts may contribute to demonstrating the neuroprotective effect and its molecular mechanism. In the present study, it was observed that GK treatment alleviated the increased expression of MCU induced by Aβ *in vitro*, which then decreased the Ca^{2+} levels in mitochondria and eventually inhibited the apoptosis of cells. The cognitive ability of APP/PS1 mice was clearly improved, with decreased expression of MCU in the neuronal cells of the mouse brain when GK was used to treat the AD mice.

The present study had certain limitations. Only the regulatory effect of GK on Ca^{2+} levels in mitochondria by targeting MCU was investigated and further research is required to investigate the effect of GK in AD pathology. For instance, an MCU-knockout AD mouse model may require to be developed to investigate the effect of GK treatment in AD mice with MCU deficit. It is known that GK exerts multiple effects, including the regulation of inflammation (11) and inhibition of oxidative stress (12). Thus, further research is required to explore the effect of GK on the inflammatory response and oxidative stress in AD pathology. In addition, further cytology experiments should be performed to detect the pathological changes in an animal model, including the expression of ionophores, injury and repair of neurons, as well as activities of intracellular signal pathways. For instance, further research should investigate the potential regulatory effect of GK through the glycogen synthase kinase-3 (GSK-3)-related pathway, as Zhou *et al* (10) reported that GK attenuated neuronal injury through the GSK-3β-dependent pathway.

In conclusion, the present study indicated that GK inhibited MCU expression, decreasing Ca^{2+} levels in mitochondria. It is suggested that GK treatment may be a potential therapeutic strategy for AD.

Acknowledgements

Not applicable.

Funding

No funding was received.

Availability of data and materials

The datasets used and/or analyzed during the current study are available from the corresponding author on reasonable request.

Authors' contributions

HL obtained funding for the present study, performed the majority of the experiments and wrote the manuscript. JL obtained funding for the present study, designed the experiments, performed parts of the experiments and wrote the manuscript. QL and XZ performed certain parts of the experiments. YS was involved in the conception of this study. HL and JL confirm the authenticity of all the raw data. All authors read and approved the final manuscript.

Ethics approval and consent to participate

The procedures and experiments in this study were approved by the Committee on Ethics of Animal Experiments, Beijing Geriatric Hospital (Beijing, China; no. 2019134).

Patient consent for publication

Not applicable.

Competing interests

The authors declare that they have no competing interests.

References

1. Hasan TF, Hasan H and Kelley RE: Overview of acute ischemic stroke evaluation and management. Biomedicines 9: 1486, 2021.
2. Huynh TV, Davis AA, Ulrich JD and Holtzman DM: Apolipoprotein E and Alzheimer's disease: The influence of apolipoprotein E on amyloid-β and other amyloidogenic proteins. J Lipid Res 58: 824-836, 2017.
3. Michaelson DM: APOE ε4: The most prevalent yet understudied risk factor for Alzheimer's disease. Alzheimers Dement 10: 861-868, 2014.
4. Rub U, Stratmann K, Heinsen H, Turco DD, Seidel K, Dunnen WD and Korf HW: The brainstem tau cytoskeletal pathology of Alzheimer's Disease: A brief historical overview and description of its anatomical distribution pattern, evolutional features, pathogenetic and clinical relevance. Curr Alzheimer Res 13: 1178-1197, 2016.
5. Raffaello A, De Stefani D and Rizzuto R: The mitochondrial Ca(2+) uniporter. Cell Calcium 52: 16-21, 2012.
6. Granatiero V, Pacifici M, Raffaello A, De Stefani D and Rizzuto R: Overexpression of mitochondrial calcium uniporter causes neuronal death. Oxid Med Cell Longev 2019: 1681254, 2019.
7. Qiu J, Tan YW, Hagenston AM, Martel MA, Kneisel N, Skehel PA, Wyllie DJA, Bading H and Hardingham GE: Mitochondrial calcium uniporter Mcu controls excitotoxicity and is transcriptionally repressed by neuroprotective nuclear calcium signals. Nat Commun 4: 2034, 2013.
8. Moreira PI, Carvalho C, Zhu X, Smith MA and Perry G: Mitochondrial dysfunction is a trigger of Alzheimer's disease pathophysiology. Biochim Biophys Acta 1802: 2-10, 2010.
9. Fu YJ, Xiong S, Lovell MA and Lynn BC: Quantitative proteomic analysis of mitochondria in aging PS-1 transgenic mice. Cell Mol Neurobiol 29: 649-664, 2009.
10. Zhou X, Wang HY, Wu B, Cheng CY, Xiao W, Wang ZZ, Yang YY, Li P and Yang H: Ginkgolide K attenuates neuronal injury after ischemic stroke by inhibiting mitochondrial fission and GSK-3β-dependent increases in mitochondrial membrane permeability. Oncotarget 8: 44682-44693, 2017.
11. Zhang Y and Miao JM: Ginkgolide K promotes astrocyte proliferation and migration after oxygen-glucose deprivation via inducing protective autophagy through the AMPK/mTOR/ULK1 signaling pathway. Eur J Pharmacol 832: 96-103, 2018.
12. Liu Q, Li X, Li L, Xu Z, Zhou J and Xiao W: Ginkgolide K protects SHSY5Y cells against oxygenglucose deprivationinduced injury by inhibiting the p38 and JNK signaling pathways. Mol Med Rep 18: 3185-3192, 2018.
13. Chen M, Zou W, Chen M, Cao L, Ding J, Xiao W and Hu G: Ginkgolide K promotes angiogenesis in a middle cerebral artery occlusion mouse model via activating JAK2/STAT3 pathway. Eur J Pharmacol 833: 221-229, 2018.
14. Ma S, Liu X, Xun Q and Zhang X: Neuroprotective effect of ginkgolide k against H2O2-induced PC12 cell cytotoxicity by ameliorating mitochondrial dysfunction and oxidative stress. Biol Pharm Bull 37: 217-225, 2014.
15. Kilkenny C, Browne W, Cuthill IC, Emerson M and Altman DG; NC3Rs Reporting Guidelines Working Group: Animal research: Reporting in vivo experiments: The ARRIVE guidelines. Br J Pharmacol 160: 1577-1579, 2010.
16. Shao L, Dong C, Geng D, He Q and Shi Y: Ginkgolide B protects against cognitive impairment in senescence-accelerated P8 mice by mitigating oxidative stress, inflammation and ferroptosis. Biochem Biophys Res Commun 572: 7-14, 2021.
17. Livak KJ, Schmittgen TD: Analysis of relative gene expression data using real-time quantitative PCR and the 2(-Delta Delta C(T)) method. Methods 25: 402-408, 2001.
18. Mulder GB and Pritchett K: The morris water maze. Contemp Top Lab Anim Sci 42: 49-50, 2003.
19. Su R, Su W and Jiao Q: NGF protects neuroblastoma cells against beta-amyloid-induced apoptosis via the Nrf2/HO-1 pathway. FEBS Open Bio 9: 2063-2071, 2019.
20. Ding Y, Zhang H, Liu Z, Li Q, Guo Y, Chen Y, Chang Y and Cui H: Carnitine palmitoyltransferase 1 (CPT1) alleviates oxidative stress and apoptosis of hippocampal neuron in response to beta-Amyloid peptide fragment Abeta25-35. Bioengineered 12: 5440-5449, 2021.
21. Morris R: Developments of a water-maze procedure for studying spatial learning in the rat. J Neurosci Methods 11: 47-60, 1984.
22. Jafari SMS and Hunger RE: IHC optical density score: A new practical method for quantitative immunohistochemistry image analysis. Appl Immunohistochem Mol Morphol 25: e12-e13, 2017.
23. Heggland I, Storkaas IS, Soligard HT, Kobro-Flatmoen A and Witter MP: Stereological estimation of neuron number and plaque load in the hippocampal region of a transgenic rat model of Alzheimer's disease. Eur J Neurosci 41: 1245-1262, 2015.
24. Shen Y, Wang H, Sun Q, Yao H, Keegan AP, Mullan M, Wilson J, Lista S, Leyhe T, Laske C, *et al*: Increased Plasma beta-secretase 1 may predict conversion to Alzheimer's disease dementia in individuals with mild cognitive impairment. Biol Psychiatry 83: 447-455, 2018.
25. Butterfield DA, Castegna A, Lauderback CM and Drake J: Evidence that amyloid beta-peptide-induced lipid peroxidation and its sequelae in Alzheimer's disease brain contribute to neuronal death. Neurobiol Aging 23: 655-664, 2002.
26. Carrillo-Mora P, Luna R and Colin-Barenque L: Amyloid beta: Multiple mechanisms of toxicity and only some protective effects? Oxid Med Cell Longev 2014: 795375, 2014.
27. Arispe N, Pollard HB and Rojas E: Giant multilevel cation channels formed by Alzheimer disease amyloid beta-protein [A beta P-(1-40)] in bilayer membranes. Proc Natl Acad Sci USA 90: 10573-10577, 1993.
28. Abramov AY, Canevari L and Duchen MR: Changes in intracellular calcium and glutathione in astrocytes as the primary mechanism of amyloid neurotoxicity. J Neurosci 23: 5088-5095, 2003.

29. Tatebayashi Y, Takeda M, Kashiwagi Y, Okochi M, Kurumadani T, Sekiyama A, Kanayama G, Hariguchi S and Nishimura T: Cell-cycle-dependent abnormal calcium response in fibroblasts from patients with familial Alzheimer's disease. Dementia 6: 9-16, 1995.
30. Peterson C, Ratan RR, Shelanski ML and Goldman JE: Altered response of fibroblasts from aged and Alzheimer donors to drugs that elevate cytosolic free calcium. Neurobiol Aging 9: 261-266, 1988.
31. Cavallucci V, Ferraina C and D'Amelio M: Key role of mitochondria in Alzheimer's disease synaptic dysfunction. Curr Pharm Des 19: 6440-6450, 2013.
32. Perez MJ, Ponce DP, Aranguiz A, Behrens MI and Quintanilla RA: Mitochondrial permeability transition pore contributes to mitochondrial dysfunction in fibroblasts of patients with sporadic Alzheimer's disease. Redox Biol 19: 290-300, 2018.
33. Calvo-Rodriguez M, Hou SS, Snyder AC, Kharitonova EK, Russ AN, Das S, Fan Z, Muzikansky A, Garcia-Alloza M, Serrano-Pozo A, *et al*: Increased mitochondrial calcium levels associated with neuronal death in a mouse model of Alzheimer's disease. Nat Commun 11: 2146, 2020.
34. Jadiya P, Kolmetzky DW, Tomar D, Meco AD, Lombardi AA, Lambert JP, Luongo TS, Ludtmann MH, Praticò D and Elrod JW: Impaired mitochondrial calcium efflux contributes to disease progression in models of Alzheimer's disease. Nat Commun 10: 3885, 2019.
35. Calvo-Rodriguez M and Bacskai BJ: High mitochondrial calcium levels precede neuronal death in vivo in Alzheimer's disease. Cell Stress 4: 187-190, 2020.
36. Ferreiro E, Oliveira CR and Pereira CMF: The release of calcium from the endoplasmic reticulum induced by amyloid-beta and prion peptides activates the mitochondrial apoptotic pathway. Neurobiol Dis 30: 331-342, 2008.
37. Nikseresht Z, Ahangar N, Badrikoohi M and Babaei P: Synergistic enhancing-memory effect of D-serine and RU360, a mitochondrial calcium uniporter blocker in rat model of Alzheimer's disease. Behav Brain Res 409: 113307, 2021.
38. Hengartner MO: The biochemistry of apoptosis. Nature 407: 770-776, 2000.
39. Calvo-Rodriguez M, Hernando-Perez E, Nuñez L and Villalobos C: Amyloid β oligomers increase ER-mitochondria Ca 2+ cross talk in young hippocampal neurons and exacerbate aging-induced intracellular Ca 2+ remodeling. Front Cell Neurosci 13: 22, 2019.
40. Singh SK, Srivastav S, Castellani RJ, Plascencia-Villa G and Perry G: Neuroprotective and antioxidant effect of ginkgo biloba extract against ad and other neurological disorders. Neurotherapeutics 16: 666-674, 2019.
41. Shi C, Liu J, Wu F and Yew DT: Ginkgo biloba extract in Alzheimer's disease: From action mechanisms to medical practice. Int J Mol Sci 11: 107-123, 2010.
42. Nowak A, Kojder K, Zielonka-Brzezicka J, Wróbel J, Bosiacki M, Fabiańska M, Wróbel M, Sołek-Pastuszka J and Klimowicz A: The use of ginkgo biloba L. as a neuroprotective agent in the Alzheimer's disease. Front Pharmacol 12: 775034, 2021.
43. Feng Z, Sun Q, Chen W, Bai Y, Hu D and Xie X: The neuroprotective mechanisms of ginkgolides and bilobalide in cerebral ischemic injury: A literature review. Mol Med 25: 57, 2019.